Effect of Aerodynamic Blade Change of Two-Stage Axial Subsonic Turbine on Design Point

Mahmood Adami, Behrooz Shahriari*, Ali Zamani Gharaghoushi
Department of Mechanical Engineering,
Malek Ashtar University of Technology, Iran
E-mail: adami@mut-es.ac.ir, shahriari@mut-es.ac.ir*, alzghh@gmail.com
*Corresponding author

Received: 20 November 2018, Revised: 2 January 2019, Accepted: 6 May 2019

Abstract: In this research for reducing the effect of losses and increasing the efficiency, the bowing in the rotor and stator blades is used. In one mode rotor blades are curved and in other one, stator blades are curved. The amount of rotor loss, due to changes in the thickness of the trailing edge and operating rotational speed, have been investigated. To confirm the accuracy of the results, a turbine stage whose experimental results are available is modeled and numerical results have been compared with experimental results that indicate acceptable compliance. The turbulence model k-w-SST is used to solve turbulent flow. The positive bowing, creates a pressure gradient from the two ends of the blade towards the center of the blade, which leads to the directing of the secondary flows toward the center of the blade. This reduces the losses in the two ends of the blade and increases the loss in the middle part of the blade. Increasing the thickness of the trailing edge, as well as increasing the turbine's operating rotational speed, will increase the loss. The curved rotor increases the efficiency and mass flow and power by 0.4% and 0.5% and 0.8% respectively and the curved nozzle reduces the efficiency and power by 0.3% and 4.9% but increases the mass flow by 0.2%. It also increases the thickness of the trailing edge of the first rotor from 0.2mm to 0.9mm at 24000 rotational speed and increases the total loss by about 35%.

Keywords: Aerodynamic Blade Changes, Axial Turbine, Blade Bowing, CFD

Reference: Adami, M., Shahriari B., and Zamani Gharaghoushi, A., "Effect of Aerodynamic Blade Change of Two-Stage Axial Subsonic Turbine on Design Point", Int J of Advanced Design and Manufacturing Technology, Vol. 12/No. 2, 2019, pp. 63-73.

Biographical notes: Mahmood Adami was born in 1959. He received the BSc, MSc and PhD degrees in mechanical engineering from University of Kansas in 1983, 1985 and 1990, respectively. He performed many industrial and academic projects and education in the fields of aerospace propulsion systems design. **Behrooz Shahriari** was born in Isfahan, Iran in 1975. He received his BSc in mechanical engineering and MSc and PhD degrees in aerospace engineering from Malek Ashtar University of Technology in 2002, 2012 and 2016, respectively. He performed some industrial and academic projects and education in the fields of aerospace propulsion systems design. **Ali Zamani Gharaghoushi** was born in Isfahan, Iran in 1990. He received his BSc in mechanical engineering and MSc in aerospace engineering from Malek Ashtar University of Technology in 2013 and 2017, respectively. He performed projects in the fields of gas turbines and other aerospace propulsion systems.

1 INTRODUCTION

Turbine and compressor are two important components of gas turbines, and their actions have a great effect on engine performance. One of the important components in rotary machines is secondary flows that play a very important role [1]. Many researches have been done to control these flows. The concept of curved blades was published in 1961 by Ditch [2]. Thenceforth many researches have been done on turbine and compressor blades [3-12]. Generally, about half of the losses in the rotary axial machines are related to the boundary layer of the two ends of the blade [13-14]. Therefore, in new designs, engine scientists try to reduce the loss in these areas [15]. The design of high efficiency turbines requires an accurate understanding of the aerodynamic losses generated due to the complex 3-D viscous flow through the turbine [16]. The losses are categorized as follows and the sources of loss are shown in "Fig. 1".

-Profile loss: this loss is due to the production of the boundary layer due to the viscous flow effects. The development of the boundary layer depends on the blade geometry that can eventually lead to separation.

-Secondary flows losses: these losses are formed in the boundary layer of the two ends of the blade, where, due to the pressure gradient between the low and high pressure surfaces of the blade, the circulation flow is generated. Due to the mixing of the secondary flows and the mainstream, vortices are generated.

-Tip clearance losses: these losses are formed in the clearance between the blade and the shell. Clearance causing leakage, and mixing the leakage flow and the mainstream flow, lead to vortex formation. The total pressure loss coefficient in the stator and the rotor is determined using equation (1) and (2).

$$YN = (P01-P02) / (P02-P2) \quad (1)$$

$$Yp = (P02\ rel-P03\ rel) / (P01\ rel-P3) \quad (2)$$

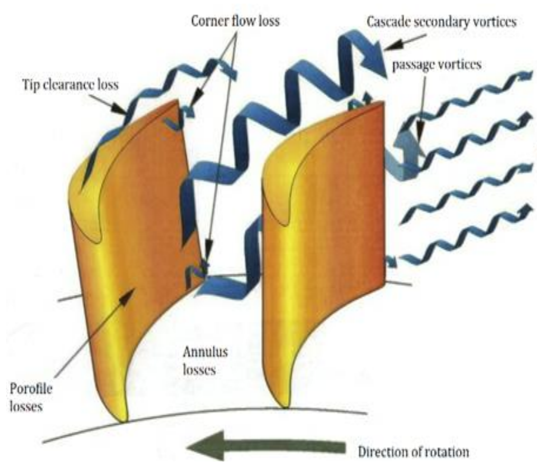

Fig. 1 Turbine losses source [9].

Lots of researches have been done on the effects of blade geometry changing on the gas turbine performance. In some cases, the effect aerodynamic deformations are positive and in some cases negative. Some of the deformations that can be mentioned are dihedral, swipe, twist, and curvilinear blade. All of this has been done in the past research. But how these changes are applied in different research is the point of differentiation between different researches.

In this research a two-stage turbine have been investigated. Some of the turbine features are given in "Table 1". Two modes are investigated. In the first mode, the rotors are curved, but the stators remain without any change, and in the second case, the stators are curved and the rotors remain without any change. Several cases have been investigated in this work. In this research it is tried to examine a particular special mode and examine the effect of the curvature of rotors or stators on the turbine separately.

Table1 Some important features of the turbine [18]

Number of stator 1 blades	43
Number of rotor 1 blades	75
Radius of rotor 1 in hub	132.5 mm
Radius of rotor 1 in tip	195 mm
Rotor1 tip clearance	0.3125 mm
Stator1 length in leading edge	122.58 mm
Stator1 length in trailing edge	63.493 mm
Rotor 1 length in leading edge	63.751mm
Rotor 1 length in trailing edge	64.86 mm
Number of stator 2 blades	61
Number of rotor 2 blades	55
Radius of stator 2 in hub	130 mm
Radius of rotor 2 in tip	122 mm
Rotor2 tip clearance	0.3125 mm
Stator2 length in leading edge	69.8 mm
Stator2 length in trailing edge	83.7 mm
Rotor 2 length in leading edge	86.5 mm
Rotor 2 length in trailing edge	89.6 mm

Figure 2 shows how changes are performed on blades. Also in a separate study, the effect of two different operating rotational speeds and blade trailing edge thickness changes, on the pressure loss coefficient have been studied.

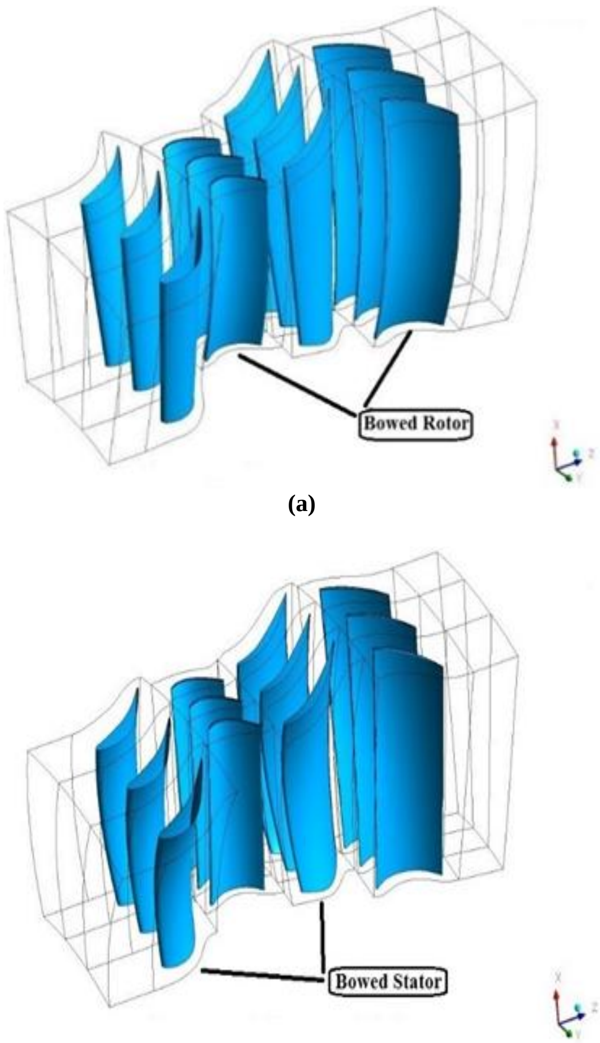

Fig. 2 Blade changes: (a): Rotors curvature and (b): Stators curvature.

2 LITERATURE REVIEW

Karabi et al [1] investigate the effect of lean, twist and blade bowing on transonic axial turbine on the design point. Their research showed that blade twisting had a great effect on the blade's performance, but the blade lean and bow had a little effect on the turbine performance. Breugelmans [3] and shang [4] experimental researches showed that the bow and lean had a great impact on the development of secondary flows between compressor blades and for the blade bowing, there was a decrease in corner separation. Fischer et al. [17] investigated the effect of blade bowing on the performance of a four-stage axial flow compressor and showed that, stator bowing removes the corner separation, increases static pressure, total pressure and total efficiency. Chen [12] by applying the curvature on a part of the fan blade, concluded that the curvature reduced the separation, and the efficiency of the fan has increased with curvature at the design point and the pressure ratio increased by 11%.

Zheng et al [15] to reduce the losses of the two ends of the blade, have investigated the effect of changing the geometry of two ends of the blade on the axial compressor performance. They applied three changes at the end of the blade. They found that the end of the blade changing, reduces the losses of the two ends of the blade, and dihedral leads to reduce the blade force at the two ends, while the sweep not only reduces the shock waves but also controls the penetration of the boundary layer in a radial direction. All of this, modifies the distribution of the blade load both in the radial direction and in the axial direction.

However, decreasing the losses at the end of the blade causes increasing the loss in the middle section. Therefore, the way to apply changes in the blade geometry is important in order to achieve the optimal loss distribution; and this depends on how we want to transform it. As seen in previous research, each of the various changes affects a particular section of the blade. As well as the characteristics of the machine, including the height of the blades, the operating range and others, can also affect the depth and amount of deformation effect. The work done in this study is based on a particular turbine with its own functional characteristics, and deformations are different from previous works. In one case, the rotor blades are bow shape and in other cases only nozzle blades are bow shape.

3 NUMERICAL SIMULATION AND GRID GENERATION

In this paper the definition of the blade curvature is the airfoils in the direction of the blade-blade, related to stacking line have been changed. In "Fig. 3" suction side and pressure side, have been shown by SS and PP respectively. The curvature angle is defined as the angle, between the stacking line and the radial direction. In this study, only a 15-degree curvature has been used. In one mode, this curvature is applied to the rotors and in the other case it is applied to the stators. Positive curvature means the curvature of the blade towards the pressure side.

To solve the turbulence flow inside a turbine, it is necessary to discrete the solution limited area into points where continuity, momentum and energy equations can be solved numerically for these points. Due to specific geometric characteristics, and also for better matching of turbine surfaces, O-Grid is used [19]. There are various parameters for verifying the quality of grid structure that are represented in this research. Among them, we can point out the aspect ratio, control volumes, deviation angle and number of nods near the walls to calculate the boundary layer with high accuracy.

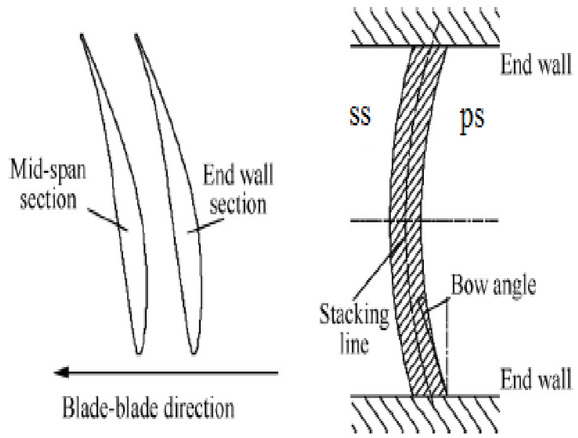

Fig. 3 Blade bowing.

Independency of the network is also have done, which indicates the independence of the results, from the number of nods used, “Fig. 4”. The boundary conditions used in the numerical researches, should be similar to real and experimental conditions [19]. All the simulations are based on steady state and there is no transition condition. For output, the static pressure condition is applied. For walls non- slip condition, the condition is repeated for blade surfaces, and for the pages between rows, mixing plan mode used. Navier stokes (RANS) equations are solved. Discretization for the mass component is based on the way in which Mr. Majamdar [20] has been done. For the convective component in the Navier Stokes equations, and also in the turbulence model, the first order and second order numerical states are available. For the momentum equation, the second order is used. For the turbulence model, the shear stress transport (SST), developed by Manter, due to good results in turbomachinery has been used. Equations governing the viscous flow, are mass conservations, momentum and energy which are given in equations (3), (4), and (5) respectively. According to the reference [21], for the number of repetitions, two limitations can be applied. One is the number of repetitions, and the other one is the remainder of the equations, which are 200 and 10^{-5}. Figure 5 shows the remainder of solving equations in numerical order.

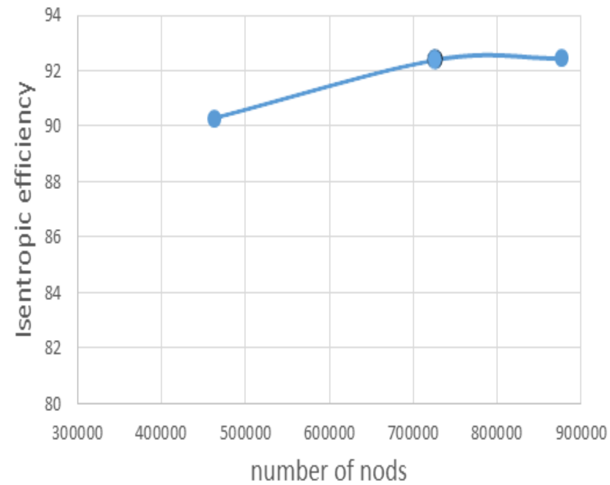

Fig. 4 Effect of grid size on efficiency.

$$\frac{\partial p}{\partial t} + \nabla .(pU) = 0 \qquad (3)$$

$$\frac{\partial}{\partial t}(\rho U) + \nabla .(\rho UU) = -\nabla \mathrm{p} + \nabla .\, \sigma_{vis} \qquad (4)$$

$$\frac{\partial}{\partial t}\left[\rho\left(e + \frac{1}{2}U^{z}\right)\right] + \nabla .\left[\rho\left(e + \frac{1}{2}U^{z}\right)U\right] = -\nabla .(pU) + \nabla(\sigma_{vis}.U) + \nabla .(\mathrm{k}\nabla \mathrm{T}) \qquad (5)$$

To solve the above relations, need formulas (6) to (9):

$$\sigma_{vis} = -\frac{2}{3\mu}(\nabla .U) + \mu(\nabla U + (\nabla U)^{T}) \qquad (6)$$

$$p = \rho RT \qquad (7)$$

$$e = C_v T \qquad (8)$$

$$C_v = \frac{R}{r_i - 1} \qquad (9)$$

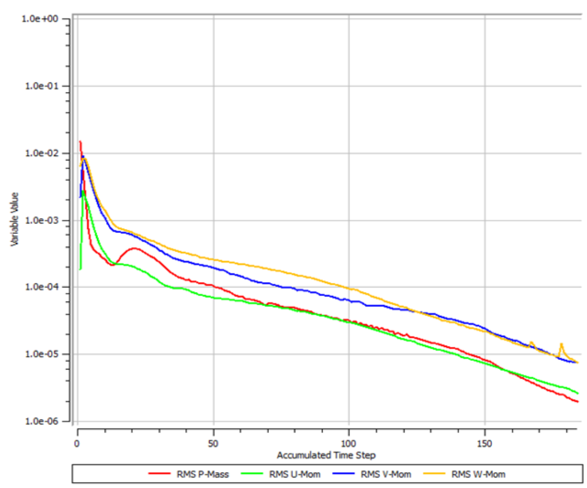

Fig. 5 Equations residuals.

4 MODEL VALIDATION

In order to validate the model used, a model with the availability of experimental results is used. The sample is a 4 stage turbine [22]. In this research, the fourth stage that the mass flow rate and rotor speed according to the nominal condition are 7.8 kg/s and 7500 rpm, has been used. Figure 6 shows how to setup the fourth stage of this turbine. Considering the effect of the boundary layer with the creation of a denser network and the flow analysis and satisfaction of the conditions in the turbine, there is a good agreement between the results in the experimental and numerical conditions. According to availability of some results in the experimental state, such as the nozzle outlet speed, the nozzle outlet angle, the outlet speed of the rotor and the outlet angle of the rotor, were also numerically investigated. Figures 7 to 10 show a comparison between the above items.

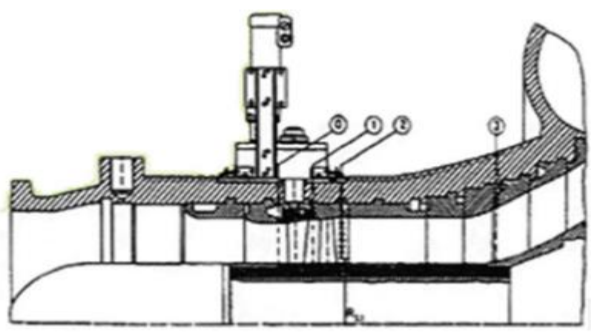

Fig. 6 Fourth stage of the turbine [22].

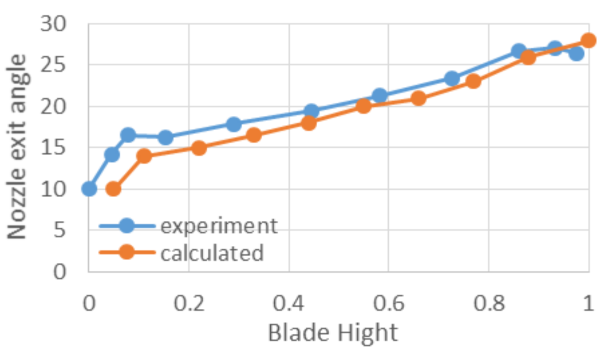

Fig. 7 Nozzle exit angle.

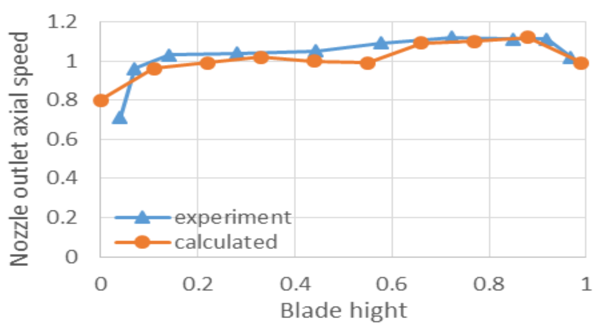

Fig. 8 Nozzle outlet speed.

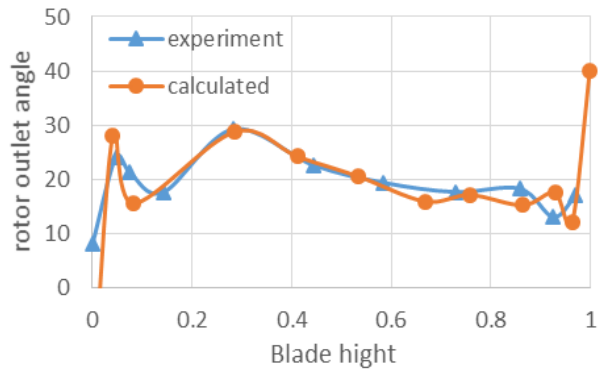

Fig. 9 Rotor outlet angle.

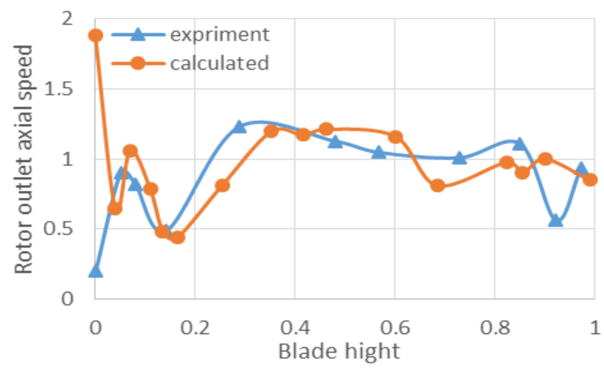

Fig. 10 Rotor exit angle.

5 ANALYSIS OF RESULTS

Figures 11 and 12 show the total pressure at two heights, 10, and 90%, for all three modes, without change, curved stator and curved rotor. The total pressure reflects energy and decrease in total pressure means loss.

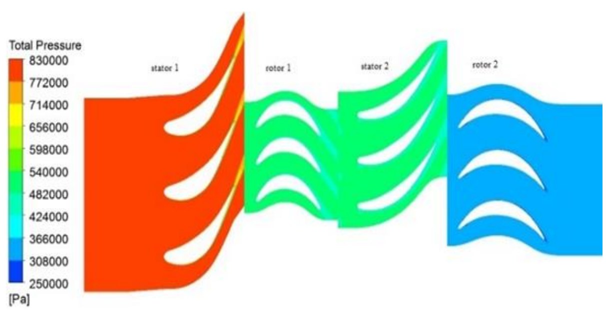

(a): Without change

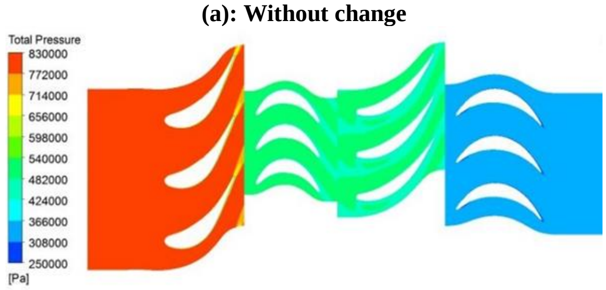

(b): Curved stator

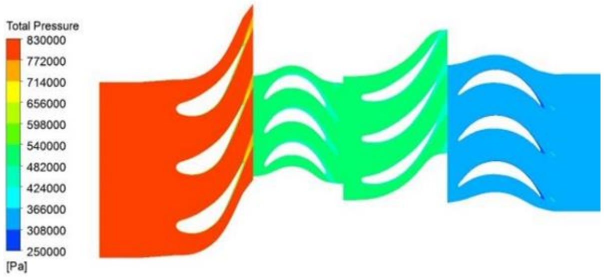

(c): Curved rotor

Fig. 11 Total pressure contour at 10% blade height for three modes.

At 10% blade height, the total pressure loss has been increased in stator curvature, "Fig. 11b", and the amount of loss in stator 2 is evident. In the rotor curvature ("Fig. 11c"), the amount of loss in the ends of the first rotor has somewhat decreased. At 90% height ("Fig. 12") the stator curvature has reduced the losses in the middle of the blades of the rotor, but the rotor curvature has increased the losses in rotor 1.

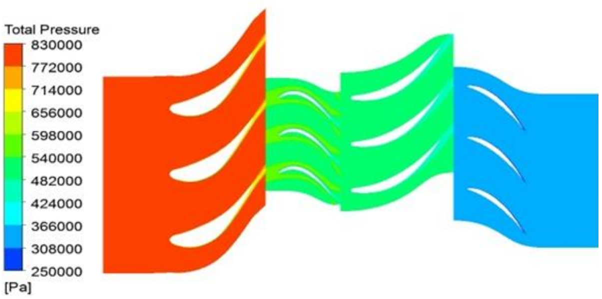

(a): Without change

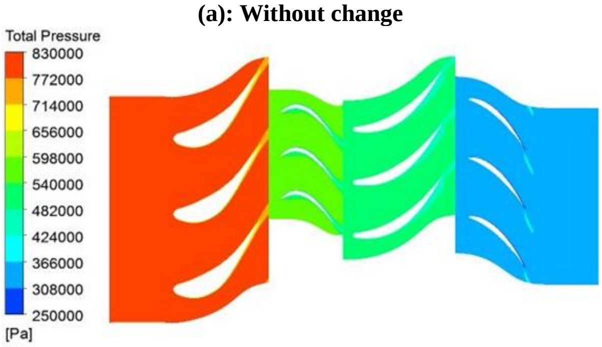

(b): Curved stator

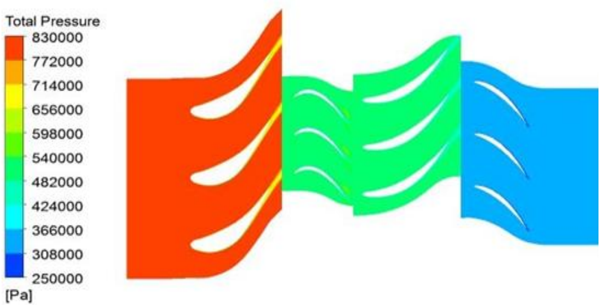

(c): Curved rotor

Fig. 12 Total pressure contour at 90% blade height for three modes.

The flow at the two ends of the blades is complex. Therefore, the methods for improving in these areas can have a significant effect on overall engine performance [1]. Figures 13 and 14 show the contour of static entropy in three sections for each blade. Looking at "Fig. 13" and comparing, the increase or production of entropy occurs in a stator with curvature. The vortices of the tip region are increased and since the curvature of the blade produces strong vortices at the end of the blade and after trailing edge [23], the vortices change the inlet flow angle of the next stage and these changes lead to change the flow distribution on the next stage. This can increase the losses on the next stage. But for rotor curvature, "Fig. 13c", the intensity of vortices caused by the tip flow, is reduced. This means reducing the losses in this area. Figure 14 also shows the same for rotor 2. By comparing "Figs. 14a, and 14c", the amount of entropy production in the curved rotor has decreased. In the rotor change mode, both the rotor1 and the rotor 2, have decreased the loss in the tip region. Although when the stators are changed, due to the change in the flow distribution, the flow angle in the inlet of the rotors has changed, which cause a decrease in the tip area losses. Entropy generation at the end of the hub, is due to vortices in this area.

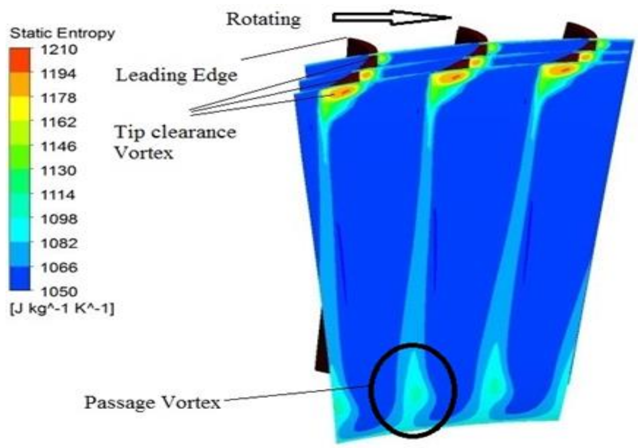

(a): Without change

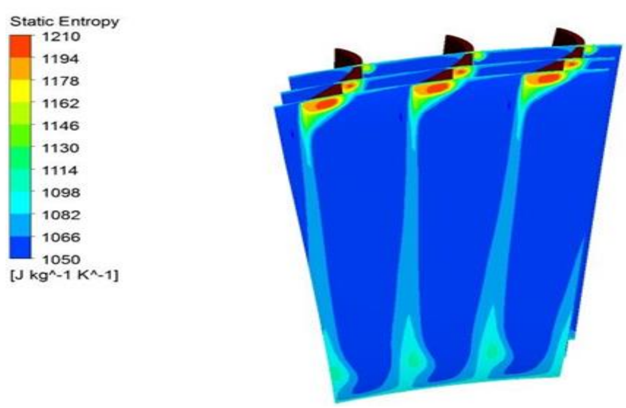

(b): Curved stator

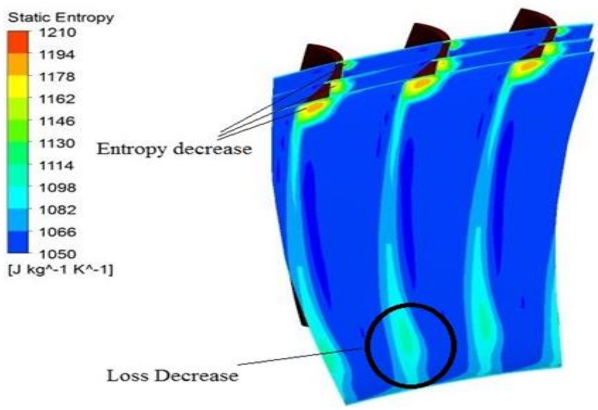

(c): Curved rotor

Fig. 13 Entropy contour for rotor 1.

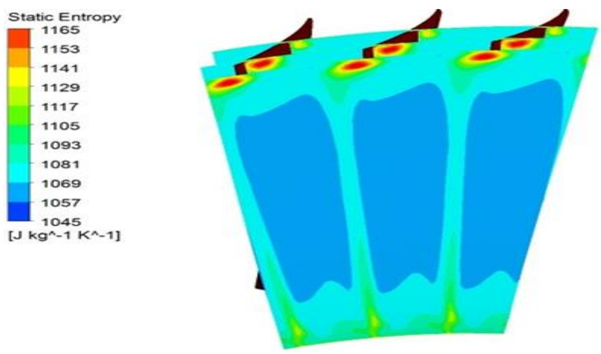

(a): Without change

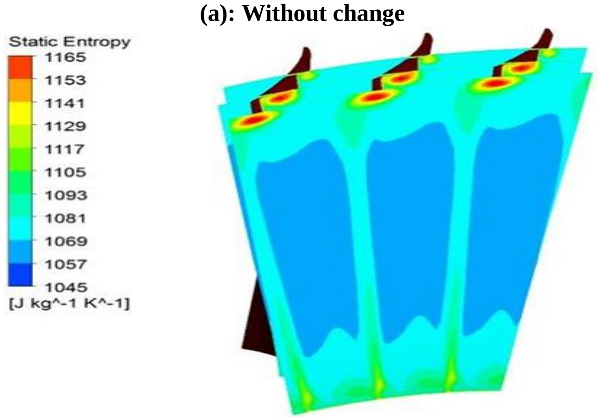

(b): Curved stator

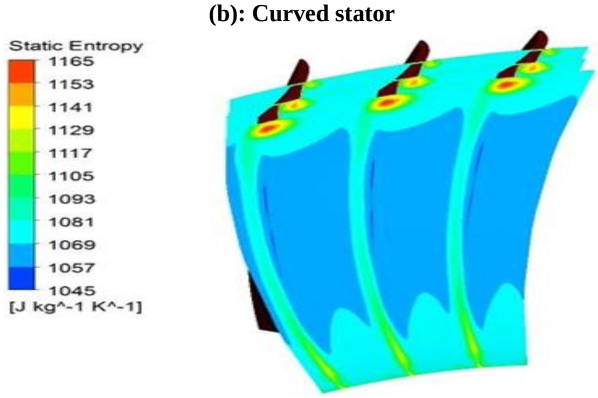

(c): Curved rotor

Fig. 14 Entropy contour for rotor 2.

Figure 15 shows stream lines at the hub, for rotor1 and 2. Different vortices formed in the blade's root end are finally joined together at the end of the blade's suction side, forming a vortex called passage vortex. This vortex usually comes upper from the boundary layer of the root portion and enters the mainstream. The blade geometry changes can affect these vortices and change their intensity and position. In curved blades, low energy fluid from the two ends of the blade is displaced to the center of the blade due to the pressure difference in the radial direction [23]. Figures 15a, and 15b show the rotor 1 and 2 blades without change. By comparing these with the curvature stator ("Fig. 15c and Fig. 15d"), there is no change in displacement at vortex height. This means that the stator's curvature is not significantly affected by the position of the rotor's hub vortex. But in comparison with "Figs 15e and 15f", the change in the position of the vortices is quite visible. The vortices on both the rotor 1 and 2 move in the radial direction, and this is due to the same force that was created from the two ends of the blade toward the mid-span. The concentration of the vortices in the two ends of the blade reduces the losses at the end of the blade, but the number of losses in the mid-span increases.

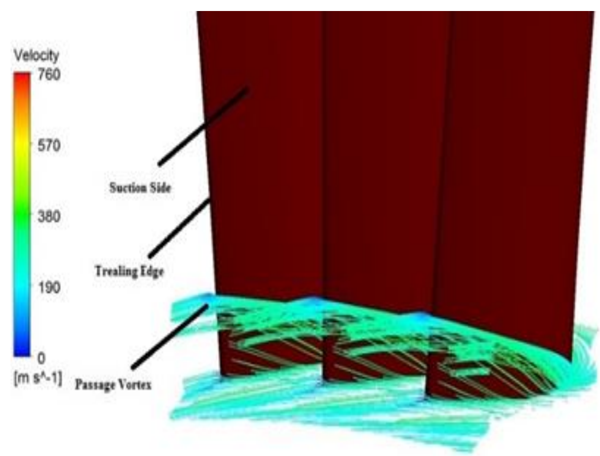

(a): Rotor 1 without change

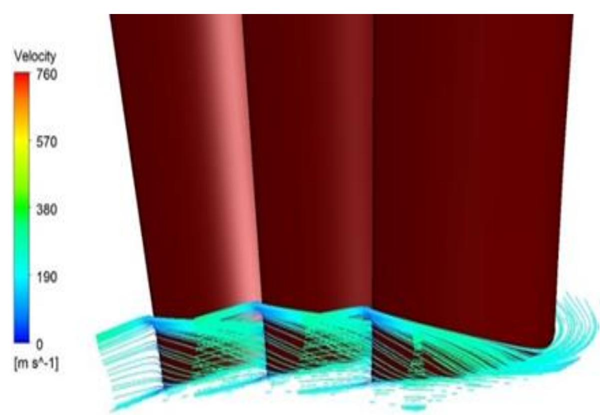

(b): Rotor 2 without change

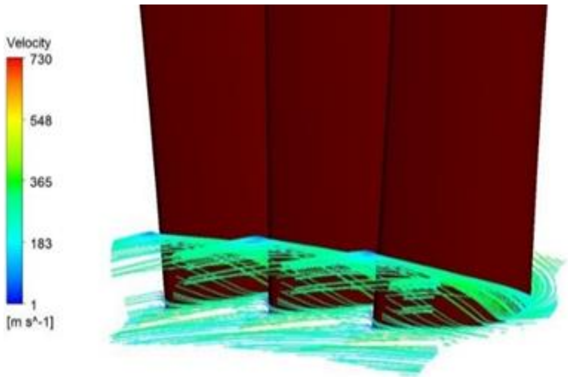

(c): Curved stator (rotor 1)

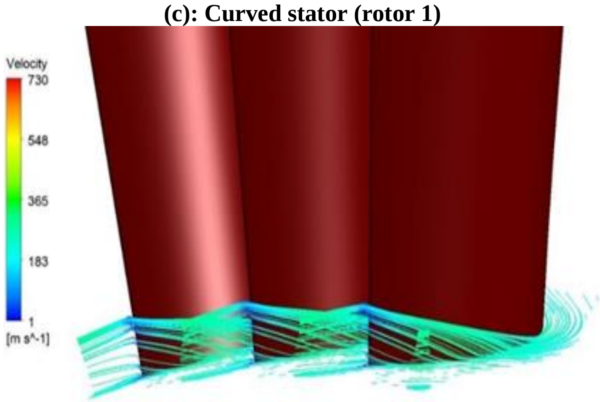

(d): Curved stator (rotor 2)

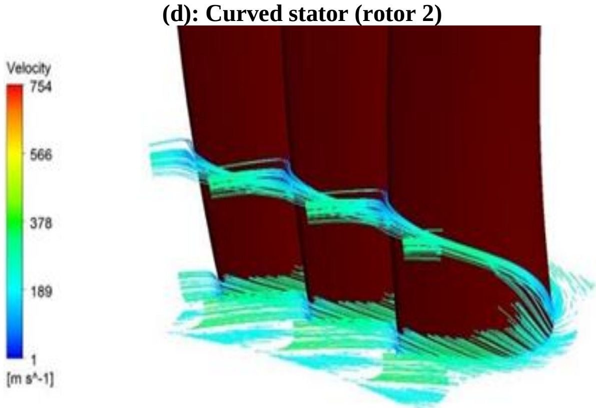

(e): Curved rotor (rotor 1)

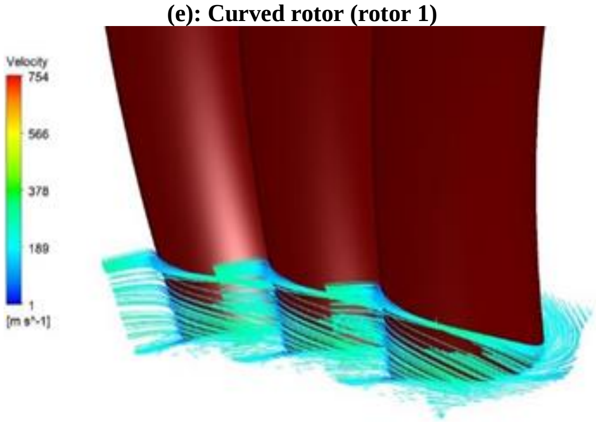

(f): Curved rotor (rotor 2)

Fig. 15 Stream lines at the hub of rotor 1 and 2.

One of the features of the curved blades is the reduction of the pressure difference between the suction side and pressure side at the two ends of the blade [24]. As a result, the blade load decreases at the two ends but it increases in the mid-span. Reduction loading at the two ends of the blade reduces the intensity of the vortices formed in this area, which, as a result, losses are reduced. Figure 16 shows the static entropy at the stator 1 and 2 outlets. With respect to the above- mentioned points and with a look at “Fig. 16d”, the reducing of the losses in the two ends of the stator is significant. Also the amount of the losses in the mid-span has increased in curvature mod.

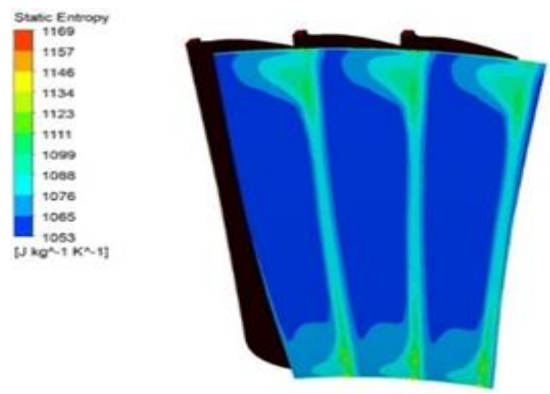

(a): Stator 2 outlet without change

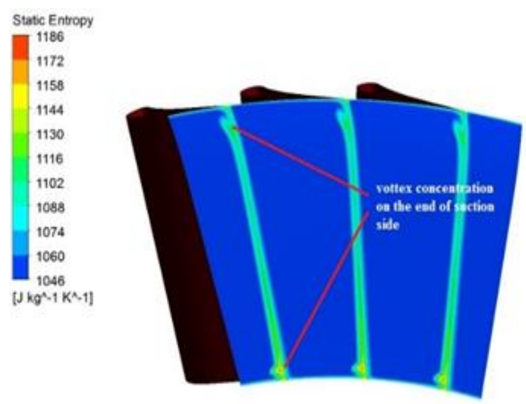

(b): Stator1 outlet without change

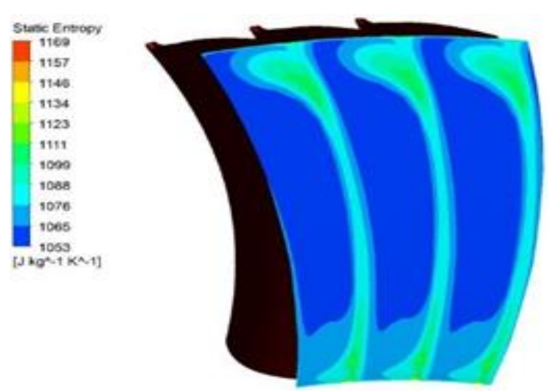

(c): Stator 2 outlet in stator curvature

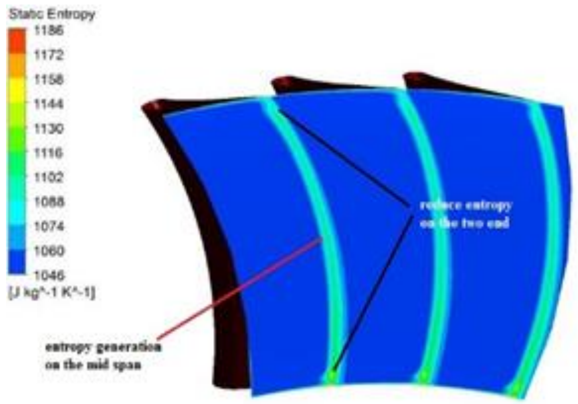

(d): Stator 1 outlet in stator curvature

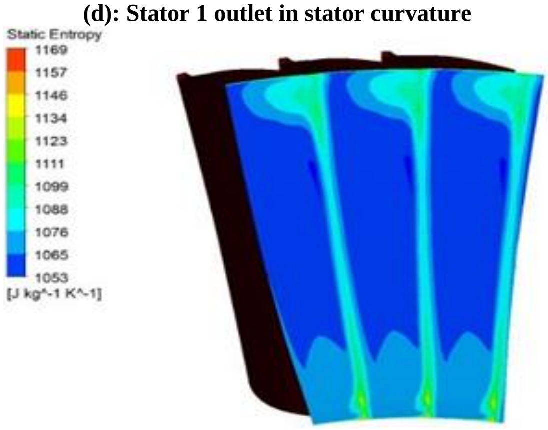

(e): Stator 2 in rotor curvature

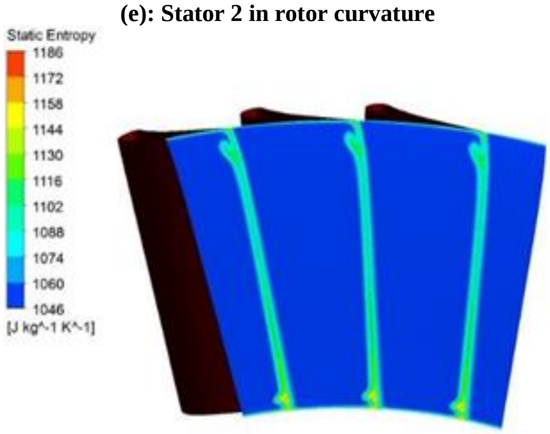

(f): Stator 1 outlet in rotor curvature

Fig. 16 Static entropy at stator 1 and 2 outlets.

$$\eta = \frac{T_{t-out} - T_{t-in}}{T_{t-in}(pr^{(\gamma-1)/\gamma} - 1)} \tag{11}$$

In this section, three parameters of the turbine; efficiency, mass flow rate and power are investigated. Isentropic efficiency is determined using equation (11). As shown in “Fig. 17”, mass flow increased in both cases, while the turbine power and efficiency increased only in rotor curvature mode. Therefore, it can be concluded that the rotor curvature improved turbine performance and reduces the losses in a different region, which ultimately lead to increased turbine efficiency and power.

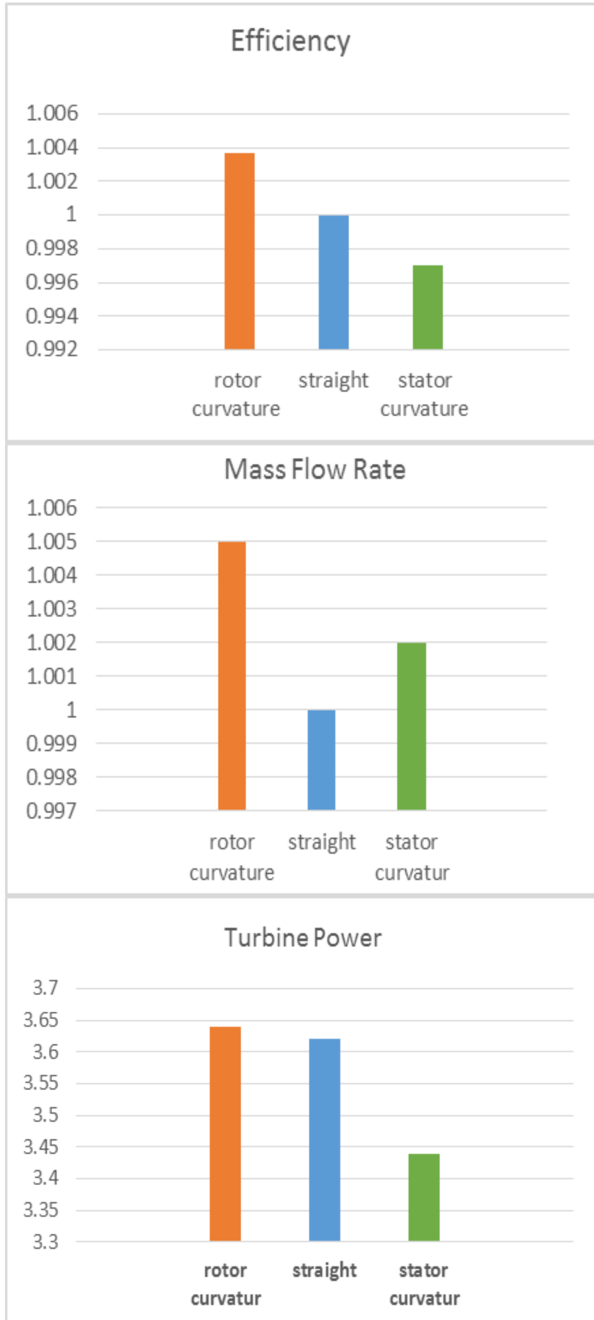

Fig. 17 Comparison of the efficiency, power and mass flow rate of the turbine.

Figure 18 shows the total pressure loss coefficient for rotor 1 for two different rotational speed and different thickness of the trailing edge. As seen, increasing the thickness of the trailing edge, increases the loss. Also, with increasing the rotational speed of the rotor, the amount of loss increase.

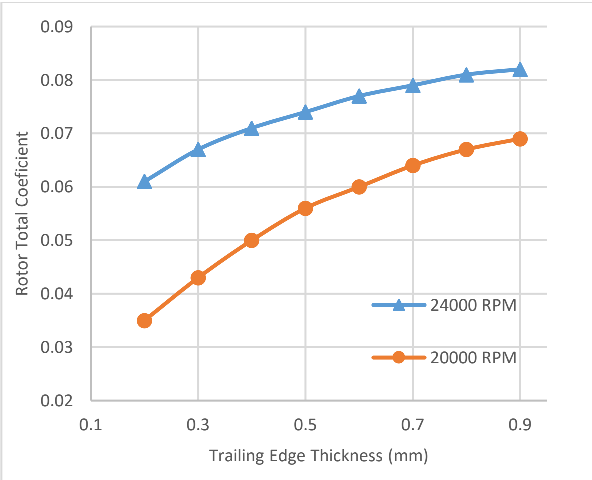

Fig. 18 Total pressure loss coefficient for rotor 1.

6 CONCLUSION

In this research, a two-stage sub sonic turbine with a high aspect ratio was investigated. In two modes; one curvature of the rotor blades in both stages and the other, the curvature of the stator blades in both stages were investigated. The total pressure loss coefficient was also compared with variations in the thickness of the trailing edge, in two different rotational speeds. The results are as follows.

1- Positive curvature in the rotor blades reduces the losses resulting from the tip clearance vortices. The losses due to passage vortices in the root portion also decreased.
2- positive curvature produces a pressure gradient from the two ends of the blade toward the center, where this pressure gradient generates a force in the same direction and transmits vortices from the two ends to the mid-span. Thereby reducing the losses on the two ends of the blade and increasing in the mid span
3- comparison of the streamlines at the two ends of the blade shows that in positive curvature, vortices are stretch to the center.
4- The turbine power and efficiency have increased only in the rotor curvature. But the mass flow has increased in both rotor and stator curvature modes. It can be concluded that the rotor curvature can have a better effect on reducing the losses which can be due to the higher losses in the rotor.
5- The increase in the total pressure loss coefficient has a direct relation to the trailing edge thickness and with the increase in the thickness of the trailing edge, the losses also increase. Increasing the turbine rotational speed will also increase the loss coefficient.

REFERENCES

[1] Karrabi,H., Rezasoltani, M., The Effect of Blade Lean, Twist and Bow on the Performance of Axial Turbine at Design Point, No. 54877, pp. 965-972, 2011.

[2] M. Deich, M., Gubarev, A., Filipov, G., and Wang, Z. C., A New Method of Profiling the Guide Vane Cascades of Turbine Stages with Small Diameter-Span Ratio, Teploenergetika, Vol. 8, pp. 42-46, 1962.

[3] Breugelmans, F. A. H., Carels, Y., and Demuth, M., Influence Of Dihedral on the Secondary Flow in a Two-Dimensional Compressor Cascade, Journal of Engineering for Gas Turbines and Power, Vol. 106, No. 3, pp. 578-584, 1984.

[4] Shang, E., Wang, Z. Q., and Su, J. X., The Experimental Investigations on the Compressor Cascades With Leaned and Curved Blade, No. 78880, pp. V001T03A018, 1993.

[5] Weingold, H. D., Neubert, R. J., Behlke, R. F., and Potter, G. E., Bowed Stators: An Example of CFD Applied to Improve Multistage Compressor Efficiency, Journal of Turbomachinery, Vol. 119, No. 2, pp. 161-168, 1997.

[6] Fischer, A., Riess, W., and Seume, J. R., Performance of Strongly Bowed Stators in a Four-Stage High-Speed Compressor, Journal of Turbomachinery, Vol. 126, No. 3, pp. 333-338, 2004.

[7] Tan, C., Yamamoto, A., Mizuki, S., and Chen, H., Influences of Blade Bowing on FlowFields of Turbine Stator Cascades, AIAA Journal, Vol. 41, No. 10, pp. 1967-1972, 2003.

[8] Tan, C., Yamamoto, A., Chen, H., and Mizuki, S., FlowField and Aerodynamic Performance of a Turbine Stator Cascade with Bowed Blades, AIAA Journal, Vol. 42, No. 10, pp. 2170-2171, 2004/10/01, 2004.

[9] Tan, C Zhang, H. Chen, H., and Yamamoto, A., Blade Bowing Effect on Aerodynamic Performance of a Highly Loaded Turbine Cascade, Journal of Propulsion and Power, Vol. 26, No. 3, pp. 604-608, 2010/05/01, 2010.

[10] Schobeiri, M. T., Suryanarayanan, A., Jermann, C., and Neuenschwander, T., A Comparative Aerodynamic and Performance Study of a Three-Stage High Pressure Turbine With 3-D Bowed Blades and Cylindrical Blades, No. 41707, pp. 1237-1246, 2004.

[11] Hassan Vand, M., Wang, S., Numerical Study of the Effects of Bowed Blades on Aerodynamic Characteristics in a High Pressure Turbine, No. 47306, pp. 487-496, 2005.

[12] L. Chen, L., Liu, X. J., Yang, A. L., and Dai, R., Flow Performance of Highly Loaded Axial Fan with Bowed Rotor Blades, IOP Conference Series: Materials Science and Engineering, Vol. 52, No. 4, pp. 042005, 2013.

[13] Koch,L. S. C., Loss Sources and Magnitude in Axial Flow Compressor, ASME J, pp. 354-363, 1976.

[14] Wisler, D. C., Loss Reduction in Axial-Flow Compressors Through Low-Speed Model Testing, Journal of Engineering for Gas Turbines and Power, Vol. 107, No. 2, pp. 354-363, 1985.

[15] Zheng, X., Li, Z., Blade-End Treatment to Improve the Performance of Axial Compressors: An Overview, 2016.

[16] Ennil, A. B., Al-Dadah, R., Mahmoud, S., Rahbar, K., and AlJubori, A., Minimization of Loss in Small Scale Axial Air Turbine Using CFD Modeling and Evolutionary Algorithm Optimization, Applied Thermal Engineering, Vol. 102, pp. 841-848, 2016/06/05/, 2016.

[17] Freeman,C., Effect of Tip Clearance Flow on Compressor Stability and Engine Performance, 2018.

[18] Bini, R., Colombo, D., Large Multistage Axial Turbines, Energy Procedia, Vol. 129, pp. 1078-1084, 2017/09/01/, 2017.

[19] Lindquist Whitacker, L. H., Tomita, J. T., and Bringhenti, C., An Evaluation of the Tip Clearance Effects on Turbine Efficiency for Space Propulsion Applications Considering Liquid Rocket Engine Using Turbopumps, Aerospace Science and Technology, Vol. 70, pp. 55-65, 2017/11/01/, 2017.

[20] Majumdar, S., Role of Underrelaxation in Momentum Interpolation for Calculation of Flow with Nonstaggered Grids, Numerical Heat Transfer, Vol. 13, No. 1, pp. 125-132, 1988/01/01, 1988.

[21] Chima, R., Liou, M. S., Comparison of the AUSM+ and H-CUSP Schemes for Turbomachinery Applications, Fluid Dynamics and Co-Located Conferences in: 16th AIAA Computational Fluid Dynamics Conference, Eds.: American Institute of Aeronautics and Astronautics, 2003.

[22] Groschup, G., Strömungstechnische Untersuchung einer Axialturbinenstufe im Vergleich Zum Verhalten Der Ebenen Gitter Ihrer Beschaufelung: Dissertation, University of Hanover, 1977.

[23] Zhongqi, L. S. W., Wenyuan, X., Aerodynamic Calculation of Turbine Stator Cascade with Curvilinear Leaned Blades and Some Experimental Results, in 5th International Symposium on Air Breathing Engine, 1981.

[24] Wang, S., Wang, Z., and Feng, G., Numerical Simulation of 3D Flow Field Structure in Turbine Cascade With Bowed Blades, No. 78507, pp. V001T03A064, 2001.